Macromolecules

Article

Cite This: Macromolecules 2019, 52, 7430−7438

pubs.acs.org/Macromolecules

Detailed Approach to Investigate Thermodynamically Controlled Supramolecular Copolymerizations

Lafayette N. J. de Windt,[†,‡] Chidambar Kulkarni,[†,‡] Huub M. M. ten Eikelder,[†,§] Albert J. Markvoort,[†,§] E. W. Meijer,[†,‡] and Anja R. A. Palmans*[,†,‡]

[†]Institute for Complex Molecular Systems, [‡]Laboratory of Macromolecular and Organic Chemistry, and [§]Computational Biology Group, Eindhoven University of Technology, P. O. Box 513, 5600 MB Eindhoven, The Netherlands

Supporting Information

ABSTRACT: Elucidating the microstructure of supramolecular copolymers remains challenging, despite the progress in the field of supramolecular polymers. In this work, we present a detailed approach to investigate supramolecular copolymerizations under thermodynamic control. Our approach provides insight into the interactions of different types of monomers and hereby allows elucidating the microstructure of copolymers. We select two monomers that undergo cooperative supramolecular polymerization by way of threefold intermolecular hydrogen bonding in a helical manner, namely, benzene-1,3,5-tricarboxamide (BTA) and benzene-1,3,5-tris(carbothioamide) (thioBTA). Two enantiomeric forms and an achiral analogue of BTA and thioBTA are synthesized and their homo- and copolymerizations are studied using light scattering techniques, infrared, ultraviolet, and circular dichroism spectroscopy. After quantifying the thermodynamic parameters describing the homopolymerizations, we outline a method to follow the self-assembly of thioBTA derivatives in the copolymerization with BTA, which involves monitoring a characteristic spectroscopic signature as a function of temperature and relative concentration. Using modified types of sergeants-and-soldiers and majority-rules experiments, we obtain insights into the degree of aggregation and the net helicity. In addition, we apply a theoretical model of supramolecular copolymerization to substantiate the experimental results. We find that the model describes the two-component system well and allows deriving the hetero-interaction energies. The interactions between the same kinds of monomers (BTA−BTA and thioBTA−thioBTA) are slightly more favorable than those between different monomers (BTA−thioBTA), corresponding to a nearly random copolymerization. Finally, to study the interactions of the monomers at the molecular level, we perform density functional theory-based computations. The results corroborate that the two-component system exhibits a random distribution of the two monomer units along the copolymer chain.

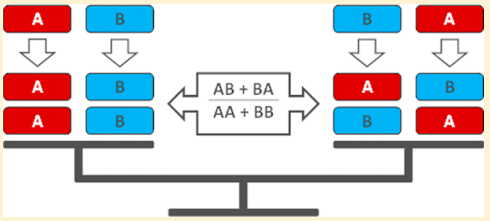

INTRODUCTION

"Much of our knowledge of the reactivities of monomers, free radicals, carbocations, and carboanions in chain copolymerization comes from copolymerization studies. The behavior of monomers in copolymerization reactions is especially useful for studying the effect of chemical structure on reactivity."[1] This statement in Odian's work "Principles of Polymerization" highlights the importance of copolymerization studies in understanding and eventually controlling chain copolymerization reactions. In principle, the approaches outlined by Odian can also be applied to study supramolecular copolymerization processes, that is, polymerization reactions driven by the formation of noncovalent interactions. For supramolecular copolymerizations, it is equally important to understand the effect of chemical structure on noncovalent interactions. Although many examples of supramolecular copolymerization have been reported, obtaining alternating, statistical, or random copolymerizations by judicious choice of monomers and reaction conditions remains elusive.[2]

Understanding the mechanism of a supramolecular polymerization is an important step toward relating the structure and property. For supramolecular homopolymerizations, a large body of work has resulted in a thorough understanding of different mechanisms of polymerization and structure−mechanism correlations.[3−5] For example, two main mechanisms have been distinguished, namely, the isodesmic and cooperative mechanisms. In an isodesmic supramolecular polymerization, the equilibrium constant of an association step involving a monomer and supramolecular polymer is independent of the length of the polymer.[6] For a cooperative polymerization, the equilibrium constant is dependent on length. When the length of an aggregate exceeds a certain critical length, the association steps are thermodynamically more favorable, corresponding to the growth of a polymer and elongation phase of the polymerization.[7−13]

Another important feature of a supramolecular polymerization is that the process can be thermodynamically[14−22] or kinetically controlled.[23−29] For thermodynamically controlled processes, polymerization occurs in the equilibrium state and rapidly assumes a new equilibrium state when internal and

Received: July 19, 2019
Revised: September 10, 2019
Published: September 26, 2019

DOI: 10.1021/acs.macromol.9b01502
Macromolecules 2019, 52, 7430−7438

external factors, such as concentration and temperature, change. Examples of thermodynamically controlled alternating,[14−19] random[20,22] and block[21] copolymerizations have been reported, which typically rely on molecular recognition processes between donor and acceptor groups through ionic, charge-transfer, or hydrogen-bonding interactions.

Although many supramolecular homopolymerizations have been performed, in light of Odian's work, studying noncovalent interactions between different kinds of monomers may afford an alternative approach to relate the structure and property. Copolymerization studies can therefore be complementary to homopolymerization studies. In this work, we present a detailed approach to elucidate thermodynamically controlled, cooperative supramolecular copolymerizations of monomers with similar interacting motifs. First, we determine the thermodynamic parameters of the homopolymerizations of the monomers. Next, we investigate the copolymerization in detail by performing conventional and modified types of sergeants-and-soldiers and majority-rules experiments. These experiments have been pioneered by Green and co-workers to understand conformational preferences in dynamic helical polymers[30,31] and were later extended to assess amplification of supramolecular chirality in dynamic supramolecular aggregates.[32] Mixing enantiomers of a supramolecular monomer together is typically referred to as the majority-rules experiment, whereas mixing achiral monomers with chiral enantiopure analogues constitutes a sergeants-and-soldiers experiment. Finally, theoretical modeling and density functional theory (DFT)-based computations are applied to obtain quantitative information on the interactions between different monomers. We anticipate that studying other systems following the approach outlined here will contribute to elucidating the principles of supramolecular copolymerization.

RESULTS

Molecular Design, Synthesis, and Characterization. To gain insight into supramolecular copolymerization processes, we opted for a pair of monomers with similar chemical structures but different interacting motifs. Therefore, benzene-1,3,5-tricarboxamide (BTA) and benzene-1,3,5-tris(carbothioamide) (thioBTA) derivatives were chosen because these monomers differ only in the atoms constituting the amide and thioamide groups (Scheme 1a). Despite their similar chemical structures, amide and thioamide groups show different hydrogen-bonding abilities.[33−35] As a result, different types of copolymers can in theory be formed, such as self-sorted, blocky, random, and alternating (Scheme 1b). In addition, we changed the structure of the alkyl chains of the monomers. Thereby, we can simultaneously study the effects of different hydrogen-bonding groups and different alkyl chains on the supramolecular copolymerization. The synthesis of the monomers was reported previously, but it was further optimized in this work (see the Supporting Information for details).[36,37] All monomers were obtained in high purity as evidenced by ^{1}H- and ^{13}C-nuclear magnetic resonance spectroscopy, matrix-assisted laser desorption/ionization time-of-flight mass spectrometry, and infrared (IR) spectroscopy (Figures S1−S20).

Scheme 1. (a) Chemical Structures of BTA and thioBTA Derivatives Studied in This Work; (b) Different Types of Supramolecular Copolymers That Can in Theory be Formed, Consisting of BTA and thioBTA Derivatives

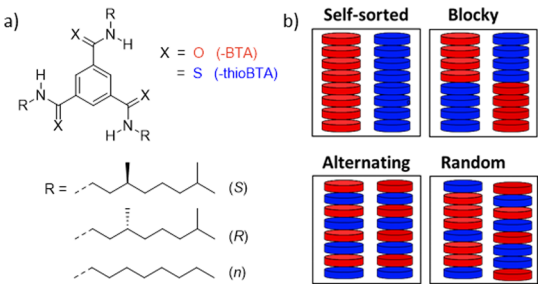

Formation of Supramolecular Polymers Stabilized by Intermolecular Hydrogen Bonding. To investigate if the BTA and thioBTA derivatives assemble into supramolecular polymers by intermolecular hydrogen bonding, we first applied IR spectroscopy and light scattering techniques. Solutions of ***n*-BTA** and ***n*-thioBTA** in methylcyclohexane (MCH) with the same total concentration of monomer were mixed at different volume-to-volume (v/v) ratios to vary the relative concentrations of the monomers. At these conditions, the majority of the monomers is present as aggregated species, which are in equilibrium with a minor fraction of the monomers present as free monomers.

The results obtained from IR spectroscopy are shown in Figure 1a and Table S1. For ***n*-BTA**, the N−H stretching and amide II bands are positioned around 3240 and 1560 cm^{-1}, respectively, whereas for ***n*-thioBTA**, the bands are positioned around 3180 and 1544 cm^{-1}, respectively. Furthermore, for ***n*-BTA**, the amide I band is a doublet with peaks positioned around 1630 and 1646 cm^{-1}, whereas for ***n*-thioBTA**, the amide I band is absent due to the absence of carbonyl groups. The positions of the N−H stretching and amide II bands measured for the solutions of ***n*-BTA** and ***n*-thioBTA** are indicative of intermolecular hydrogen-bonding interactions.[36,37] Mixing the solutions of ***n*-BTA** and ***n*-thioBTA** results in a change of the intensity and position of the N−H stretching band that is proportional to the relative concentration of the monomers.

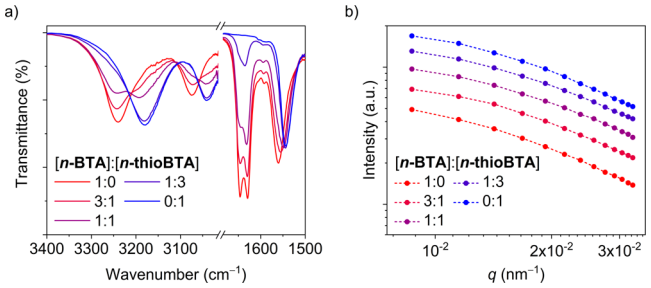

Figure 1. (a) Partial Fourier-transform infrared spectra and (b) scattering intensity as a function of the magnitude of the scattering wavevector (q) measured for solutions of ***n*-BTA** and ***n*-thioBTA** at various v/v ratios of the monomers. Solutions were prepared in MCH at c_{tot} = 2.0 mM, and measurements were performed at 20 °C.

Figure 1b summarizes the results obtained from static light scattering. The magnitudes of the scattering intensity measured for the solutions of ***n*-BTA** and ***n*-thioBTA** differ from each other, which is attributed to the larger polarizability of sulfur atoms relative to oxygen atoms.[37] In contrast, the scattering profiles are similar. Specifically, the intensities scale with q^{-1} at values of q ranging from 2 × 10^{-2} to 3 × 10^{-2} nm^{-1} and begin to scale with q^{0} at values of q smaller than 1 × 10^{-2} nm^{-1}.

DOI: 10.1021/acs.macromol.9b01502
Macromolecules 2019, 52, 7430−7438

Table 1. Overview of the Thermodynamic Parameters Describing the Supramolecular Homopolymerizations[a]

	ΔH_e kJ·mol^{-1}	ΔH_n kJ·mol^{-1}	ΔS J·mol^{-1}·K^{-1}	ΔG_e[b] kJ·mol^{-1}	ΔG_n[b] kJ·mol^{-1}	σ[b]
***S*-BTA**	−59.9	>−29.9[c]	−90.5	−33.4	>−3.4[c]	$<10^{-6}$
***n*-BTA**	−60.1	−40.6	−90.5	−33.6	−14.1	3.3×10^{-4}
***S*-thioBTA**	−65.7	−50.4	−102.6	−35.6	−20.3	1.9×10^{-3}
***n*-thioBTA**	−62.9	−47.2	−90.7	−36.4	−20.6	1.5×10^{-3}

[a]The thermodynamic parameters were obtained by analyzing data acquired from UV−vis spectroscopy experiments. [b]Changes in Gibbs free energy of elongation (ΔG_e) and nucleation (ΔG_n), and the cooperativity factor (σ) are reported for a temperature of 293 K. [c]Value could not be determined accurately.

When mixing the solutions, the magnitude of the intensity changes proportionally to the relative concentrations of the monomers, whereas the scattering profile remains the same. The scattering profiles indicate the presence of structures with a cylindrical shape and a size larger than the experimentally accessible length scale (about 600 nm). This result is corroborated by dynamic light scattering (Figure S21).

When mixing the solutions, the positions of the N−H stretching and amide II bands and the scattering profile remain nearly the same. Hence, also in mixtures of ***n*-BTA** and ***n*-thioBTA**, supramolecular polymerization occurs, indicating that mixing the two molecular systems does not adversely affect polymerization. However, the results obtained for the mixtures of the solutions are linear combinations of the separate components. Therefore, although the results obtained from IR spectroscopy and light scattering techniques indicate that the mixtures of BTA and thioBTA derivatives assemble into one-dimensional polymers through intermolecular hydrogen bonding, we cannot conclude whether the mixtures assemble either into homopolymers or into copolymers.

Thermodynamic Analysis of Supramolecular Homopolymerizations. Before investigating the supramolecular copolymerization in more detail, we first revisit the homopolymerization of the monomers. As reported previously, cooperative polymerizations can be described in terms of thermodynamic parameters defining the nucleation (ΔH_n, ΔS) and elongation phases (ΔH_e, ΔS). We here apply temperature-dependent circular dichroism (CD) and ultraviolet (UV) spectroscopy to follow the net helicity and the degree of aggregation, respectively, as a function of temperature. In addition, we apply a one-component equilibrium model to quantify the thermodynamic parameters of the homopolymerizations.[7,8,38] Details are given in the Supporting Information (Figures S22−S30 and Tables S2−S5). Table 1 summarizes the results of the thermodynamic analysis obtained by analyzing data from UV spectroscopy experiments. This approach allows a comparison of achiral ***n*-BTA** and ***n*-thioBTA** with chiral analogues. We also performed a van't Hoff analysis, which corroborates the values of the parameters for the elongation phase (see the Supporting Information for details).

The results show remarkable relationships between the type of monomer and values of the thermodynamic parameters. First, when comparing monomers with amide groups, the value of the cooperativity factor (σ) is smaller for the monomers with dimethyloctyl chains than for the monomer with octyl chains. The smaller value of σ indicates that the polymerization of ***S*-BTA** is more cooperative than the polymerization of ***n*-BTA**. The difference in the cooperativity factor between ***S*-BTA** and ***n*-BTA** can be attributed to a difference in dihedral angle between the amide and benzene groups.[5,39] For the BTA derivatives, the magnitude of the angle depends on the structure of the alkyl side chains. Because the cooperativity factor is similar for ***S*-thioBTA** and ***n*-thioBTA**, we propose that the dihedral angle between the thioamide and benzene groups is independent of the structure of the side chains, which can be explained by a relative large distance between neighboring, assembled monomers.

Furthermore, the values of the change in Gibbs free energy of elongation (ΔG_e) are similar to one another, indicating similar thermodynamic stabilities of the interactions of ***S*-BTA** and ***n*-BTA**. Second, when comparing monomers with thioamide groups, the results show opposite relationships. The values of ΔG_e are slightly less negative for ***S*-thioBTA** than for ***n*-thioBTA**, whereas the values of σ are similar to one another. Thus, in contrast to monomers with amide groups, the interactions of ***S*-thioBTA** are less stable than the interactions of ***n*-thioBTA** whereas the degrees of cooperativity of the polymerizations of ***S*-thioBTA** and ***n*-thioBTA** are similar to one another. Finally, when comparing monomers with amide and thioamide groups, the values of ΔG_e are more negative for the thioBTA derivatives whereas the values of σ are smaller for the BTA derivatives. Thus, the interactions of monomers with thioamide groups are more stable, whereas the polymerization of monomers with amide groups is more cooperative. To summarize, despite their similar chemical structures, the monomers show interesting differences in their supramolecular homopolymerizations.

Sergeants-and-Soldiers Principle in Supramolecular Copolymerizations of BTA and thioBTA Derivatives. To investigate if the BTA and thioBTA derivatives assemble into supramolecular copolymers, we performed conventional and modified "sergeants-and-soldiers" experiments, using chiral and achiral monomers with identical and different interacting motifs, respectively.[30,40] The experiments were performed with two types of sergeants, ***S*-BTA** and ***S*-thioBTA**, and two types of soldiers, ***n*-BTA** and ***n*-thioBTA**. However, we focus on mixtures containing soldiers of ***n*-thioBTA**. This system was chosen since only ***n*-thioBTA** absorbs at wavelengths larger than 300 nm. As a result, the contribution of the soldiers to the CD spectra can be easily recognized upon mixing ***n*-thioBTA** with sergeants of ***S*-BTA**, which is not the case for ***n*-BTA** and ***S*-thioBTA** (Figure S31). Following previous reports of our group,[41,42] we initially varied the fraction of sergeants and kept the total concentration of sergeants and soldiers constant (Figures 2b, S32 and S33b). This approach works well when the optical properties of sergeants and soldiers closely resemble each another. However, when mixtures of BTA and thioBTA derivatives are used, the CD and UV spectra of the monomers are very different (Figure S34). Varying the fraction of sergeants changes the concentration of soldiers in the experiments, making the interpretation more demanding. As a result, we opted to vary the concentration of sergeants while keeping the concentration of soldiers constant (Figures 2a and

DOI: 10.1021/acs.macromol.9b01502
Macromolecules 2019, 52, 7430−7438

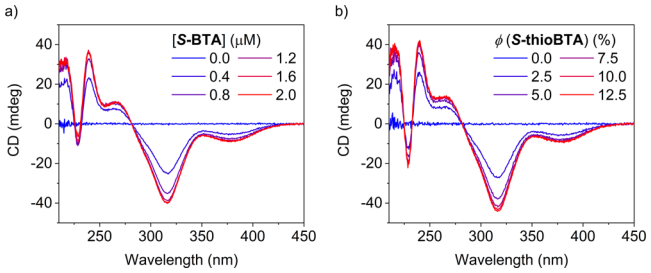

Figure 2. CD spectra measured for solutions of ***n*-thioBTA** and (a) ***S*-BTA** or (b) ***S*-thioBTA**. Sergeants-and-soldiers experiments were performed at either (a) various concentrations of sergeants and a fixed concentration of soldiers of 20 μM or (b) various fractions of sergeants and a fixed total concentration of sergeants and soldiers of 20 μM. Solutions were prepared in MCH, and spectra were measured at 20 °C.

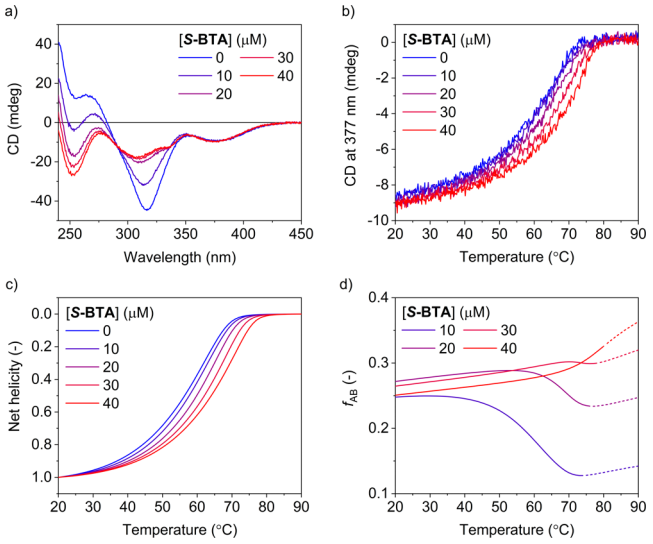

Figure 3. (a) CD spectra at 20 °C and (b) CD effect at 377 nm as a function of temperature measured for ***S*-thioBTA** at 20 μM and ***S*-BTA** at 0, 10, 20, 30, or 40 μM. (c) Net helicity with respect to ***S*-thioBTA** (= $([M]_{thio} - [P]_{thio})/[\textbf{S-thioBTA}]_{tot}$) and (d) fraction of hetero-interactions (f_{AB}) as a function of temperature simulated for the copolymerization of ***S*-BTA** and ***S*-thioBTA** (parameters: ΔH_{AA} = −65.7 kJ·mol^{-1}, ΔS_{AA} = −102.6 J·mol^{-1}·K^{-1}, NP_A = 15.3 kJ·mol^{-1}, MP_A = 0.3 kJ·mol^{-1}, ΔH_{BB} = −59.9 kJ·mol^{-1}, ΔS_{BB} = −90.5 J·mol^{-1}·K^{-1}, NP_B = 30 kJ·mol^{-1}, MP_B = 0.3 kJ·mol^{-1}, r_{AB} = 0.96, ΔS_{AB} = −96.6 J·mol^{-1}·K^{-1}).

S33a). Hereby, the contributions of the sergeants and soldiers to the CD spectra are more easily distinguished easily from each other, and the bias in helical sense induced by the sergeant can be quantified more easily (Figure S35).

Figure 2a shows that at a fixed concentration of soldiers, the addition of ***S*-BTA** induces a CD effect in the region where ***n*-thioBTA** absorbs, indicating an interaction between the two kinds of monomers. The CD effect reaches a constant value of −40 mdeg at 317 nm around a concentration of ***S*-BTA** of 1.2 μM, which corresponds to a fraction of sergeants of 6%. These values are in line with the conventional sergeants-and-soldiers experiment, mixing ***n*-thioBTA** with ***S*-thioBTA**, where the CD effect reaches −44 mdeg at 317 nm around a fraction of sergeants of 8% (Figure 2b).

The results of the sergeants-and-soldiers experiments evidence that the BTA and thioBTA derivatives form supramolecular copolymers that comprise both types of monomers. For supramolecular copolymers consisting mainly of the soldier ***n*-thioBTA**, the bias in helical sense induced by a sergeant is similar for ***S*-BTA** and ***S*-thioBTA**. However, for copolymers consisting mostly of ***n*-BTA**, the same type of sergeant ***S*-BTA** induces a stronger bias than the other type of sergeant ***S*-thioBTA** (Figure S35).

Supramolecular Copolymerization of *S*-BTA and *S*-thioBTA. To study the copolymerization of BTA and thioBTA derivatives in more detail, we first focus on the copolymerization of ***S*-BTA** and ***S*-thioBTA**. These monomers were chosen because they possess the same alkyl chains and assemble only into M-helical polymers at 20 °C. The sergeants-and-soldiers experiments described above illustrate that keeping the concentration of thioBTA derivatives constant makes the interpretation of results more straightforward than keeping the total concentration of BTA and thioBTA derivatives constant.[20] Therefore, we prepared solutions at a constant concentration of ***S*-thioBTA** (20 μM) and various concentrations of ***S*-BTA** (0−40 μM) in MCH and studied the dependence of the copolymerization process on the concentration of ***S*-BTA**.

Figure 3a shows CD spectra measured at 20 °C (corresponding UV spectra are shown in Figure S36a). The band around 315 nm shows clear changes when changing the concentration of ***S*-BTA**. With increasing concentration from 0 to 25 μM, this band decreases in intensity and shifts to smaller wavelengths. In contrast, these changes are not observed at higher concentration of ***S*-BTA** (25−40 μM). Furthermore, the band around 375 nm does not show a dependence on the concentration of ***S*-BTA**.

These results indicate that the band around 315 nm is sensitive to the nature of hydrogen-bonding interactions. In the absence of ***S*-BTA**, these interactions occur only between thioamide groups. However, in the presence of ***S*-BTA**, hydrogen bonding occurs also between amide and thioamide groups, leading to the observed changes. The fact that these changes are observed only at low concentrations of ***S*-BTA** (0−25 μM) hints at a strong driving force for hydrogen-bonding interactions between amide and thioamide groups. The band around 375 nm does not show these changes, indicating that this band is less sensitive to the nature of the hydrogen-bonding interactions. We attribute this band to the helical preference of the supramolecular polymers of ***S*-BTA** and ***S*-thioBTA**, which reflects the net helicity with respect to ***S*-thioBTA**, $([M]_{thio} - [P]_{thio})/[\textbf{S-thioBTA}]_{tot}$.

Next, we performed temperature-dependent measurements by monitoring the CD effect at 377 nm upon decreasing the temperature of the solutions (Figure 3b). The wavelength of 377 nm was chosen because it probes the net helicity with respect to ***S*-thioBTA**. At low concentrations of ***S*-BTA** (10−20 μM), the CD curves show a similar shape and temperature of elongation (T_e) as the curve measured in the absence of ***S*-BTA**. In contrast, at higher concentrations of ***S*-BTA** (30−40 μM), the curves show a higher T_e and a steeper slope around T_e than the curve measured without ***S*-BTA**.

These results clearly indicate that ***S*-BTA** and ***S*-thioBTA** copolymerize. The increase in T_e upon the addition of ***S*-BTA** resembles the effect of increasing concentration in homopolymerizations. However, this effect is observed only at high concentrations of ***S*-BTA** (30−40 μM), which shows that copolymerizations with different dependencies on temperature occur at different concentrations of ***S*-BTA**. For example, at

DOI: 10.1021/acs.macromol.9b01502
Macromolecules 2019, 52, 7430−7438

high concentrations of ***S*-BTA** (30−40 μM), the copolymerizations of ***S*-BTA** and ***S*-thioBTA** occur at higher temperatures than the homopolymerization of ***S*-thioBTA**, whereas at low concentrations of ***S*-BTA** (10−20 μM), the copolymerizations occur at similar temperatures as the homopolymerization of ***S*-thioBTA**.

To gain insight into these copolymerizations, we performed simulations using a two-component equilibrium model.[43] This model is analogous to the terminal model of chain copolymerization,[1] but it assumes that monomer and supramolecular polymers are in thermodynamic equilibrium and that reactions between them are reversible. The model applied here describes the supramolecular copolymerization of two types of monomers into two types of supramolecular polymers with either M- or P-helicity. We distinguish between M- and P-helical polymers because their thermodynamic stabilities are different for chiral monomers. If the chirality of the monomers and helicity of the polymers do not match, we assign a mismatch penalty (MP) to the corresponding interactions. For example, a MP of 0.3 kJ mol^{-1} is assigned to the interactions between ***S*-thioBTA** and P-helical polymers (Scheme S1).

In this model, two different interactions are possible between different types of monomers, namely, an interaction between one monomer A and a polymer with the other monomer B as the end unit (AB-type) and an interaction between monomer B and the end unit A (BA-type). We here assume that these interactions can be described by a single parameter, r_{AB} (eq 1). This parameter is defined as the ratio of the changes in enthalpy of interactions between different types of monomers (ΔH_{AB} and ΔH_{BA}) to the changes in enthalpy of interactions between the same types of monomers (ΔH_{AA} and ΔH_{BB}). Additionally, we assume that ΔH_{AB} is equal to ΔH_{BA}. If the value of r_{AB} is greater than unity, each type of monomer preferentially interacts with the other type of monomer and as the value of r_{AB} approaches zero, monomers show an increasing preference for interacting with their own type.

$$\Delta H_{AB} = \Delta H_{BA} = r_{AB} \times (\Delta H_{AA} + \Delta H_{BB})/2 \quad (1)$$

To determine the value of r_{AB} for the copolymerization of ***S*-BTA** and ***S*-thioBTA**, we compared the measured CD effect at 377 nm (Figure 3b) and the simulated net helicity with respect to ***S*-thioBTA**. We find a good agreement between the experiments and simulations for r_{AB} = 0.96, as shown in Figure 3c. This value is slightly less than unity, which indicates that the monomers show a marginal preference for interacting with their own type.

To illustrate this preference, we computed the fraction of interactions between different types of monomers, f_{AB}, as a function of temperature (Figure 3d). Below 40 °C, the value of f_{AB} is about 0.25, which implies that one in four interactions occurs between ***S*-BTA** and ***S*-thioBTA** and suggests that the distribution of monomers along the copolymer chain is nearly random. Furthermore, at these temperatures, f_{AB} is nearly independent of temperature, which relates to the fact that the system is nearly fully aggregated, and the copolymerization is thermodynamically controlled. Above 60 °C, the situation is clearly different. At different concentration of ***S*-BTA**, f_{AB} shows different dependencies on temperature. At low concentration of ***S*-BTA** (10−20 μM), the value of f_{AB} is initially lower than 0.25, which indicates that the relative amount of ***S*-BTA** incorporated into the copolymers increases upon decreasing the temperature of the solutions. At higher concentrations of ***S*-BTA** (30−40 μM), the value of f_{AB} is already close to 0.25, which indicates that the relative amount of ***S*-BTA** incorporated into the copolymers remains nearly constant upon cooling the solutions. Finally, taking these results together, we propose that the relative large fraction of hetero-interactions computed in the simulations might explain the relative high T_e and steep slope around T_e observed in the experiments (Figure 3b).

Supramolecular Copolymerizations of Other BTA Derivatives and *S*-thioBTA. So far, we only considered the copolymerization of ***S*-BTA** and ***S*-thioBTA**, which assemble into M-helical polymers. The same combination of experiments and simulations can be applied to study other copolymerizations, in which the monomers assemble into either P-helical polymers or mixtures of M- and P-helical polymers (Schemes S2 and S3). As indicated above, it is important to identify a characteristic band that can be attributed to either the BTA or thioBTA derivative in the copolymerization, so that the hetero-interactions in the copolymerization can be followed experimentally. For ***S*-BTA** and ***S*-thioBTA**, we identified the CD effect at 377 nm as the characteristic band which probes the self-assembly of ***S*-thioBTA** in the copolymerization and described the hetero-interactions in terms of r_{AB}. To test the generality of these finding, we next focus on the copolymerizations of ***n*-BTA** and ***S*-thioBTA** and ***R*-BTA** and ***S*-thioBTA**. These BTA derivatives were chosen because they assemble into either racemic mixtures of M- and P-helical polymers (***n*-BTA**) or P-helical polymers (***R*-BTA**).

Figure 4a,b shows CD spectra measured for mixtures of ***n*-BTA** or ***R*-BTA**, respectively, and ***S*-thioBTA** (corresponding UV spectra are shown in Figure S36b,c). In comparison to ***S*-BTA**, the CD band around 315 nm shows a weaker dependence on the concentration of ***n*-BTA** and no shoulder is observed at 335 nm. For ***R*-BTA**, the band around 315 nm not only decreases in intensity and shifts to smaller wavelengths but also changes from a negative to a positive sign. Furthermore, the CD effect at 377 nm changes from −10 mdeg at 0 μM of ***R*-BTA** to 0 and +10 mdeg at 20 and 40 μM of ***R*-BTA**, respectively.

These results indicate that ***S*-thioBTA** assembles into different types of copolymers in the presence of the different BTA derivatives. Because the alkyl chains of ***S*-thioBTA** favor one type of helicity, the addition of ***n*-BTA** and ***R*-BTA** might be described by the sergeants-and-soldiers and majority-rules principle, respectively. The fact that the band around 375 nm does not show a dependence on the concentration of ***S*-BTA** or ***n*-BTA** (Figures 3a and 4a, respectively), but does show a dependence on the concentration of ***R*-BTA** (Figure 4b) suggests that only the addition of ***R*-BTA** results in the formation of copolymers with P-helicity. At 0 μM of ***R*-BTA**, only M-helical copolymers are present, whereas at 40 μM of ***R*-BTA**, only P-helical copolymers are present. Interestingly, at an equimolar amount of ***R*-BTA** (20 μM), a racemic mixture of M- and P-helical copolymers appears present. Last, for ***n*-BTA**, the absence of the shoulder at 335 nm suggests a different packing of the monomers, which reflects the different alkyl chains of ***n*-BTA** and *S*-/***R*-BTA**.

In comparison to ***S*-BTA**, the results of the temperature-dependent measurements also show differences (Figure 4c,d). At high concentrations of ***n*-BTA** (30−40 μM), the increase in T_e is less pronounced and the slope of the CD curves around T_e is more linear than in the case of ***S*-BTA** (Figure 3b). For ***R*-BTA**, the curves also change in sign. At 10 and 40 μM of ***R*-**

DOI: 10.1021/acs.macromol.9b01502
Macromolecules 2019, 52, 7430−7438

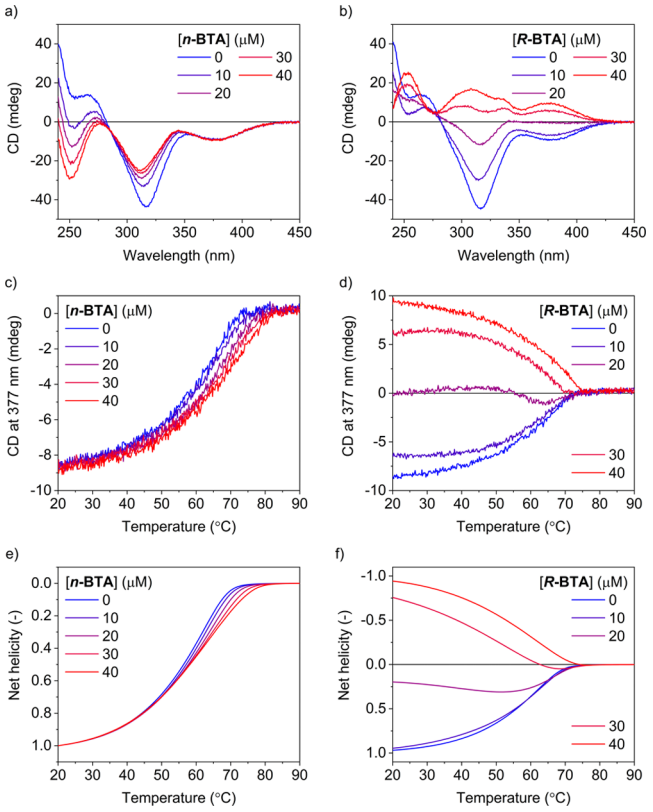

Figure 4. (a,b) CD spectra at 20 °C and (c,d) CD effect at 377 nm as a function of temperature measured for ***S*-thioBTA** at 20 μM and ***n*-BTA** or ***R*-BTA** at 0, 10, 20, 30, or 40 μM. (e,f) Net helicity with respect to ***S*-thioBTA** (= ($[M]_{thio} - [P]_{thio}$)/$[$***S*-thioBTA**$]_{tot}$) as a function of temperature predicted for the copolymerization of ***n*-BTA** or ***R*-BTA** and ***S*-thioBTA** (parameters for ***n*-BTA**: ΔH_{AA} = −65.7 kJ·mol^{-1}, ΔS_{AA} = −102.6 J·mol^{-1}·K^{-1}, NP_A = 15.3 kJ·mol^{-1}, MP_A = 0.3 kJ·mol^{-1}, ΔH_{BB} = −60.1 kJ·mol^{-1}, ΔS_{BB} = −90.5 J·mol^{-1}·K^{-1}, NP_B = 19.5 kJ·mol^{-1}, MP_B = 0 kJ·mol^{-1}, r_{AB} = 0.96, ΔS_{AB} = −96.6 J·mol^{-1}·K^{-1}; parameters for ***R*-BTA**: ΔH_{BB} = −59.9 kJ·mol^{-1}, ΔS_{BB} = −90.5 J·mol^{-1}·K^{-1}, NP_B = 30 kJ·mol^{-1}, MP_B = 0.3 kJ·mol^{-1}).

BTA, the sign of the CD effect at 377 nm is only negative and positive, respectively. Interestingly, at an equimolar amount of ***R*-BTA** (20 μM), the sign of the CD effect is initially negative and becomes positive upon decreasing the temperature of the solution. As in the case of ***S*-BTA**, at a high concentration of ***R*-BTA** (40 μM), the curve shows a higher T_e and a steeper slope around T_e than the curve measured in the absence of ***R*-BTA**.

We hypothesize that these results can be rationalized by the sergeants-and-soldiers and majority-rules principles. To test this hypothesis, we used the value of r_{AB} determined for the copolymerization of ***S*-BTA** and ***S*-thioBTA** to predict the net helicity with respect to ***S*-thioBTA** as a function of temperature for the copolymerizations of ***n*-BTA** or ***R*-BTA** and ***S*-thioBTA**. As shown in Figure 4e,f, we find a good agreement between the experiments and simulations, which demonstrates that the same value of r_{AB} can successfully describe the copolymerizations of ***S*-thioBTA** and the BTA derivatives. At 0 μM of ***R*-BTA**, only M-helical copolymers are formed upon cooling the solution, whereas at 40 μM of ***R*-BTA**, only P-helical copolymers are formed. At an equimolar amount of ***R*-BTA** (20 μM), an excess of M-helical copolymers is formed at high temperatures. This type of helicity is favored by the alkyl chains of ***S*-thioBTA**. Upon further cooling the solution, a slight excess of P-helical copolymers is formed, which is favored by the alkyl chains of ***R*-BTA**. Hence, these results suggest that the relative amount of ***R*-BTA** incorporated into the copolymers increases upon decreasing the temperature of the solution. Finally, at high concentrations of ***n*-BTA** (30−40 μM), we propose that a mixture of M- and P-helical copolymers is formed at high temperatures, which changes into M-helical copolymers at low temperatures due to the dynamic nature of the supramolecular structures (see below).

Choice of Co-monomer in Supramolecular Copolymerization of BTA Derivatives and *S*-thioBTA. So far, we simulated and predicted the net helicity with respect to ***S*-thioBTA** and computed the fraction of interactions between different types of monomers (f_{AB}). However, more insight into the copolymerizations of the BTA derivatives and ***S*-thioBTA** can be gained by constructing speciation plots[20] and copolymerization curves[21] (Figures S38−S41). Because we here described net helicity as the difference in concentrations of ***S*-thioBTA** in M- and P-helical polymers, we considered these concentrations separately to highlight differences between the different copolymerizations. At a high concentration of the BTA derivatives (40 μM), the concentration of ***S*-thioBTA** in M-helical copolymers decreases in the order of ***S*-BTA**, ***n*-BTA**, and ***R*-BTA** (Figure 5a). However, this

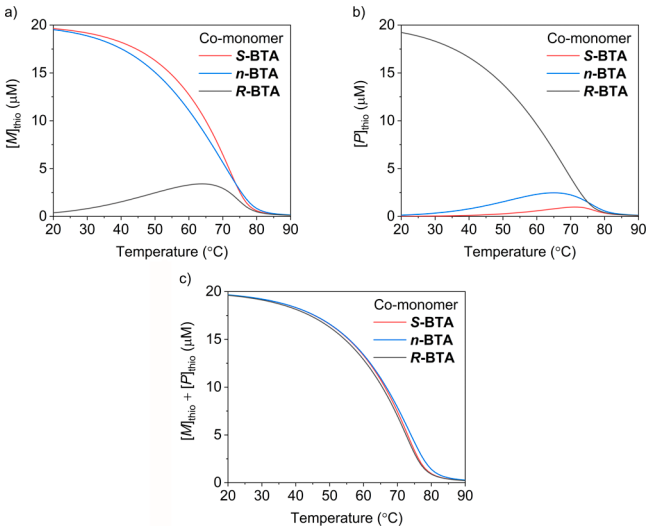

Figure 5. Concentration of ***S*-thioBTA** in (a) M-helical, (b), P-helical, and (c) both M- and P-helical copolymers as a function of temperature simulated for the copolymerizations of the BTA derivatives and ***S*-thioBTA** ($[$***S*-thioBTA**$]_{tot}$ = 20 μM, $[$***S*-/*n*-/*R*-BTA**$]_{tot}$ = 40 μM, parameters for ***S*-BTA** and ***R*-BTA**: ΔH_{AA} = −65.7 kJ·mol^{-1}, ΔS_{AA} = −102.6 J·mol^{-1}·K^{-1}, NP_A = 15.3 kJ·mol^{-1}, MP_A = 0.3 kJ·mol^{-1}, ΔH_{BB} = −59.9 kJ·mol^{-1}, ΔS_{BB} = −90.5 J·mol^{-1}·K^{-1}, NP_B = 30 kJ·mol^{-1}, MP_B = 0.3 kJ·mol^{-1}, r_{AB} = 0.96, ΔS_{AB} = −96.6 J·mol^{-1}·K^{-1}; parameters for ***n*-BTA**: ΔH_{BB} = −60.1 kJ·mol^{-1}, ΔS_{BB} = −90.5 J·mol^{-1}·K^{-1}, NP_B = 19.5 kJ·mol^{-1}, MP_B = 0 kJ·mol^{-1}).

decrease does not result from a decrease in the concentration of ***S*-thioBTA** in both M- and P-helical copolymers (Figure 5c) but coincides with an increase in the concentration of ***S*-thioBTA** in P-helical copolymers (Figure 5b). In other words, the incorporation of ***S*-thioBTA** in P-helical copolymers is promoted by choosing ***R*-BTA** (and, to a lesser extent, ***n*-BTA**) as co-monomer. This result demonstrates that the choice of co-monomer provides a way to direct the supramolecular copolymerization of ***S*-thioBTA** into either M- or P-helical copolymers.

DOI: 10.1021/acs.macromol.9b01502
Macromolecules 2019, 52, 7430−7438

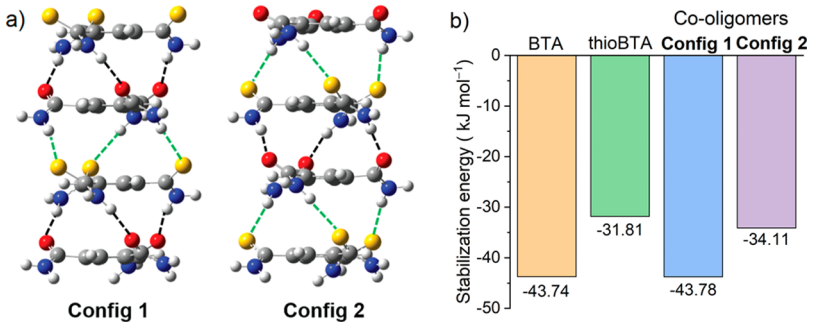

Figure 6. Computational study on oligomers of BTA and thioBTA. (a) Optimized geometry of alternating co-tetramers with different configurations (config 1 and config 2). The different kinds of hydrogen bonds involving oxygen and sulfur atoms as acceptor moieties are depicted in dashed lines with black and green color, respectively. (b) Computed basis set superposition error (BSSE)-corrected stabilization energy for homo- and co-tetramers.

Stability of BTA and thioBTA Oligomers. To understand the copolymerization of BTA and thioBTA derivatives at the molecular level, we performed DFT-based computations on model compounds (see the Supporting Information for details). Derivatives of BTA are known to form one-dimensional structures through threefold intermolecular hydrogen bonding in a helical manner, as observed through single-crystal X-ray diffraction[44] and DFT[45] studies. However, little is known about the self-assembly of thioBTA. Thus, we first performed DFT-based computations on a model compound of thioBTA. This compound also underwent intermolecular hydrogen bonding, leading to the formation of one-dimensional structures (Figure S42), similar to those observed for BTA. However, the enthalpic stability of thioBTA oligomers is substantially lower than that of BTA oligomers (Table S6).

For alternating co-oligomers of BTA and thioBTA, two configurations can be identified with different hydrogen-bonding networks, namely, one in which the majority of the hydrogen-bond acceptors are amide groups (config 1) and another in which the majority of the acceptors are thioamide groups (config 2, Figure 6a). For co-dimers, config 1 is ∼25 kJ mol^{-1} more stable than config 2 (Figure S43 and Table S7). However, for co-tetramers, this difference is only ∼10 kJ mol^{-1} (Figure 6b and Table S8), which suggests that the difference in stability between the two configurations diminishes as the size of the oligomers increases. Hence, we expect that, as the oligomer size approaches the experimental range of polymer lengths, this difference becomes vanishingly small.

Moreover, the stabilization energies of the two co-tetramers are similar to the stabilization energies of the two homo-tetramers (Figure 6b). Thus, in the absence of a strong entropic contribution to the stabilization of co-oligomers, homo- and co-oligomers have similar stabilities. Therefore, we expect that the self-assembly of BTA and thioBTA involves interactions between the same as well as different kinds of monomers with similar probabilities, corresponding to a random distribution of the monomers along the oligomer chain. This type of microstructure is in-line with the results of the theoretical modeling of the supramolecular copolymerizations (see above).

DISCUSSION

The approach outlined here to elucidate thermodynamically controlled supramolecular copolymerizations requires the use of spectroscopic techniques as well as theoretical modeling. For experiments, it is convenient to identify a diagnostic band (the CD band around 375 nm in the case of ***S*-BTA** and ***S*-thioBTA**) as a distinct signature of one of the components in the copolymerization (***S*-thioBTA**). This band needs to be independent of the concentration of the other component (***S*-BTA**). In addition, it is important to vary the concentration of this other component (***S*-BTA**) in the copolymerization while keeping the concentration of the first component (***S*-thioBTA**) constant. In this way, temperature-dependent measurements at different concentrations of the co-monomer will permit to experimentally asses the influence of the second component on the polymerization of the first component. Finally, when considering other co-monomers with different preferences for assembling into M- and P-helical polymers (***n*-BTA** and ***R*-BTA**), conflicting preferences will permit to assess to what extent the choice of co-monomer provides a way to direct the supramolecular copolymerization.

To successfully simulate copolymerization curves, the thermodynamic parameters of the homopolymerizations need to be determined first. Then, the introduction of a parameter that describes the interactions between different components (r_{AB} = 0.96 in the case of ***S*-BTA** and ***S*-thioBTA**) allows simulating copolymerization curves as a function of temperature. When the simulations are in good agreement with the experimentally obtained curves, theoretical modeling allows computing the fraction of interactions between different components ($f_{AB} \approx 0.25$) and hereby asses the microstructure of supramolecular copolymers (nearly random in the case of ***S*-BTA** and ***S*-thioBTA**).

We anticipate that the approach described here is suited to elucidate a wide range of thermodynamically controlled, cooperative supramolecular copolymerizations of monomers with similar interacting motifs. Our approach is also applicable when the self-assembly mechanisms differ or for copolymerizations that follow the majority-rules and sergeants-and-soldiers principles. Moreover, this approach is not restricted to systems under thermodynamic control, but might also be applicable to kinetically controlled supramolecular polymerizations, if appropriate kinetic models become available. We believe that generalized approaches, such as the one described here, will contribute to elucidating the principles of supramolecular copolymerization, in a similar way as has been accomplished for chain-growth copolymerizations.

DOI: 10.1021/acs.macromol.9b01502
Macromolecules 2019, 52, 7430−7438

CONCLUSIONS

In this work, we investigated the thermodynamically controlled, cooperative supramolecular copolymerization of C_3-symmetrical monomers comprising amide or thioamide groups. These monomers assemble into long, one-dimensional polymers in solution that are stabilized by intermolecular hydrogen bonding. The formation of these structures follows a cooperative mechanism, which was analyzed using a theoretical model of supramolecular polymerization. As a next step, the supramolecular copolymerization of the monomers was studied in great detail. In the copolymerization, the majority-rules and the sergeants-and-soldiers principles are operative, which provides insight into the net helicity and degree of aggregation. Additionally, modeling and DFT-based computations shows that the interaction energies of interactions between the same and different kinds of monomers are comparable to one another, which translates into a moderate fraction of interaction between different kinds of monomers. These results are indicative of a nearly random copolymerization of monomer comprising amide or thioamide groups.

A systematic study of supramolecular copolymerizations of monomers with similar interacting motifs is a useful tool to investigate the effect of chemical structure on noncovalent interactions. We anticipate that studying other systems following the approach outlined here will allow establishing structure−property relationships in supramolecular copolymerizations and may, eventually, lead to the rational design of supramolecular systems.

ASSOCIATED CONTENT

Supporting Information

The Supporting Information is available free of charge on the ACS Publications website at DOI: 10.1021/acs.macromol.9b01502.

Molecular characterization of all compounds, additional UV and CD spectroscopic data, details of the equilibrium models for supramolecular homo- and copolymerization, additional speciation plots and copolymerization curves, MATLAB scripts, and details regarding the DFT-based calculations (PDF)

Solver for mass-balance equations with two types of monomers and equilibrium model of a two-component supramolecular copolymerization of monomers A and B into two types of helical supramolecular copolymers (ZIP)

AUTHOR INFORMATION

Corresponding Author

*E-mail: a.palmans@tue.nl.

ORCID

Chidambar Kulkarni: 0000-0001-8342-9256

Huub M. M. ten Eikelder: 0000-0002-4098-0715

Albert J. Markvoort: 0000-0001-6025-9557

E. W. Meijer: 0000-0003-4126-7492

Anja R. A. Palmans: 0000-0002-7201-1548

Notes

The authors declare no competing financial interest.

ACKNOWLEDGMENTS

This work was financially supported by The Netherlands Organization for Scientific Research (ECHO grant 713.016.003) and the Dutch Ministry of Education, Culture and Science (Gravity program FMS 024.001.035).

REFERENCES

(1) Odian, G. *Principles of Polymerization*, 4th ed.; John Wiley & Sons, Inc.: Hoboken, NJ, USA, 2004.

(2) Adelizzi, B.; Van Zee, N. J.; De Windt, L. N. J.; Palmans, A. R. A.; Meijer, E. W. Future of Supramolecular Copolymers Unveiled by Reflecting on Covalent Copolymerization. *J. Am. Chem. Soc.* **2019**, *141*, 6110−6121.

(3) De Greef, T. F. A.; Smulders, M. M. J.; Wolffs, M.; Schenning, A. P. H. J.; Sijbesma, R. P.; Meijer, E. W. Supramolecular Polymerization. *Chem. Rev.* **2009**, *109*, 5687−5754.

(4) Kulkarni, C.; Balasubramanian, S.; George, S. J. What Molecular Features Govern the Mechanism of Supramolecular Polymerization? *ChemPhysChem* **2013**, *14*, 661−673.

(5) Kulkarni, C.; Meijer, E. W.; Palmans, A. R. A. Cooperativity Scale: A Structure-Mechanism Correlation in the Self-Assembly of Benzene-1,3,5-Tricarboxamides. *Acc. Chem. Res.* **2017**, *50*, 1928−1936.

(6) Martin, R. B. Comparisons of Indefinite Self-Association Models. *Chem. Rev.* **1996**, *96*, 3043−3064.

(7) Goldstein, R. F.; Stryer, L. Cooperative Polymerization Reactions. Analytical Approximations, Numerical Examples, and Experimental Strategy. *Biophys. J.* **1986**, *50*, 583−599.

(8) Zhao, D.; Moore, J. S. Nucleation-Elongation: A Mechanism for Cooperative Supramolecular Polymerization. *Org. Biomol. Chem.* **2003**, *1*, 3471−3491.

(9) Würthner, F.; Yao, S.; Beginn, U. Highly Ordered Merocyanine Dye Assemblies by Supramolecular Polymerization and Hierarchical Self-Organization. *Angew. Chem., Int. Ed.* **2003**, *42*, 3247−3250.

(10) García, F.; Viruela, P. M.; Matesanz, E.; Ortí, E.; Sánchez, L. Cooperative Supramolecular Polymerization and Amplification of Chirality in C_3-Symmetrical OPE-Based Trisamides. *Chem.—Eur. J.* **2011**, *17*, 7755−7759.

(11) Mayoral, M. J.; Rest, C.; Stepanenko, V.; Schellheimer, J.; Albuquerque, R. Q.; Fernández, G. Cooperative Supramolecular Polymerization Driven by Metallophilic Pd···Pd Interactions. *J. Am. Chem. Soc.* **2013**, *135*, 2148−2151.

(12) Cafferty, B. J.; Gállego, I.; Chen, M. C.; Farley, K. I.; Eritja, R.; Hud, N. V. Efficient Self-Assembly in Water of Long Noncovalent Polymers by Nucleobase Analogues. *J. Am. Chem. Soc.* **2013**, *135*, 2447−2450.

(13) Casellas, N. M.; Pujals, S.; Bochicchio, D.; Pavan, G. M.; Torres, T.; Albertazzi, L.; García-Iglesias, M. From Isodesmic to Highly Cooperative: Reverting the Supramolecular Polymerization Mechanism in Water by Fine Monomer Design. *Chem. Commun.* **2018**, *54*, 4112−4115.

(14) Fouquey, C.; Lehn, J.-M.; Levelut, A.-M. Molecular Recognition Directed Self-assembly of Supramolecular Liquid Crystalline Polymers from Complementary Chiral Components. *Adv. Mater.* **1990**, *2*, 254−257.

(15) Ghosh, S.; Ramakrishnan, S. Small-Molecule-Induced Folding of a Synthetic Polymer. *Angew. Chem., Int. Ed.* **2005**, *44*, 5441−5447.

(16) Colquhoun, H. M.; Zhu, Z.; Cardin, C. J.; Gan, Y.; Drew, M. G. B. Sterically Controlled Recognition of Macromolecular Sequence Information by Molecular Tweezers. *J. Am. Chem. Soc.* **2007**, *129*, 16163−16174.

(17) Florian, A.; Mayoral, M. J.; Stepanenko, V.; Fernández, G. Alternated Stacks of Nonpolar Oligo(p-Phenyleneethynylene)-BODIPY Systems. *Chem.—Eur. J.* **2012**, *18*, 14957−14961.

(18) Frisch, H.; Unsleber, J. P.; Lüdeker, D.; Peterlechner, M.; Brunklaus, G.; Waller, M.; Besenius, P. PH-Switchable Ampholytic Supramolecular Copolymers. *Angew. Chem., Int. Ed.* **2013**, *52*, 10097−10101.

(19) Narayan, B.; Bejagam, K. K.; Balasubramanian, S.; George, S. J. Autoresolution of Segregated and Mixed P-n Stacks by Stereoselective Supramolecular Polymerization in Solution. *Angew. Chem., Int. Ed.* **2015**, *54*, 13053−13057.

DOI: 10.1021/acs.macromol.9b01502
Macromolecules 2019, 52, 7430−7438

(20) Das, A.; Vantomme, G.; Markvoort, A. J.; Ten Eikelder, H. M. M.; Garcia-Iglesias, M.; Palmans, A. R. A.; Meijer, E. W. Supramolecular Copolymers: Structure and Composition Revealed by Theoretical Modeling. *J. Am. Chem. Soc.* **2017**, *139*, 7036−7044.
(21) Adelizzi, B.; Aloi, A.; Markvoort, A. J.; Ten Eikelder, H. M. M.; Voets, I. K.; Palmans, A. R. A.; Meijer, E. W. Supramolecular Block Copolymers under Thermodynamic Control. *J. Am. Chem. Soc.* **2018**, *140*, 7168−7175.
(22) Coelho, J. P.; Matern, J.; Albuquerque, R. Q.; Fernández, G. Mechanistic Insights into Statistical Co-Assembly of Metal Complexes. *Chem.—Eur. J.* **2019**, *25*, 8915.
(23) Wang, X.; Guerin, G.; Wang, H.; Wang, Y.; Manners, I.; Winnik, M. A. Cylindrical Block Copolymer Micelles and Co-Micelles of Controlled Length and Architecture. *Science* **2007**, *317*, 644−647.
(24) Ogi, S.; Sugiyasu, K.; Manna, S.; Samitsu, S.; Takeuchi, M. Living Supramolecular Polymerization Realized through a Biomimetic Approach. *Nat. Chem.* **2014**, *6*, 188−195.
(25) Ogi, S.; Stepanenko, V.; Sugiyasu, K.; Takeuchi, M.; Würthner, F. Mechanism of Self-Assembly Process and Seeded Supramolecular Polymerization of Perylene Bisimide Organogelator. *J. Am. Chem. Soc.* **2015**, *137*, 3300−3307.
(26) Kang, J.; Miyajima, D.; Mori, T.; Inoue, Y.; Itoh, Y.; Aida, T. A Rational Strategy for the Realization of Chain-Growth Supramolecular Polymerization. *Science* **2015**, *347*, 646−651.
(27) Görl, D.; Zhang, X.; Stepanenko, V.; Würthner, F. Supramolecular Block Copolymers by Kinetically Controlled Co-Self-Assembly of Planar and Core-Twisted Perylene Bisimides. *Nat. Commun.* **2015**, *6*, 7009.
(28) Zhang, K.; Yeung, M. C.-L.; Leung, S. Y.-L.; Yam, V. W.-W. Living Supramolecular Polymerization Achieved by Collaborative Assembly of Platinum(II) Complexes and Block Copolymers. *Proc. Natl. Acad. Sci. U.S.A.* **2017**, *114*, 11844−11849.
(29) Jung, S. H.; Bochicchio, D.; Pavan, G. M.; Takeuchi, M.; Sugiyasu, K. A Block Supramolecular Polymer and Its Kinetically Enhanced Stability. *J. Am. Chem. Soc.* **2018**, *140*, 10570−10577.
(30) Green, M. M.; Reidy, M. P.; Johnson, R. D.; Darling, G.; O'Leary, D. J.; Willson, G. Macromolecular Stereochemistry: The Out-of-Proportion Influence of Optically Active Comonomers on the Conformational Characteristics of Polyisocyanates. The Sergeants and Soldiers Experiment. *J. Am. Chem. Soc.* **1989**, *111*, 6452−6454.
(31) Green, M. M.; Garetz, B. A.; Munoz, B.; Chang, H.; Hoke, S.; Cooks, R. G. Majority Rules in the Copolymerization of Mirror Image Isomers. *J. Am. Chem. Soc.* **1995**, *117*, 4181−4182.
(32) Palmans, A. R. A.; Meijer, E. W. Amplification of Chirality in Dynamic Supramolecular Aggregates. *Angew. Chem., Int. Ed.* **2007**, *46*, 8948−8968.
(33) Lee, H.-J.; Choi, Y.-S.; Lee, K.-B.; Park, J.; Yoon, C.-J. Hydrogen Bonding Abilities of Thioamide. *J. Phys. Chem. A* **2002**, *106*, 7010−7017.
(34) Yanagisawa, Y.; Nan, Y.; Okuro, K.; Aida, T. Mechanically Robust, Readily Repairable Polymers via Tailored Noncovalent Cross-Linking. *Science* **2018**, *359*, 72−76.
(35) Wezenberg, S. J.; Feringa, B. L. Supramolecularly Directed Rotary Motion in a Photoresponsive Receptor. *Nat. Commun.* **2018**, *9*, 1984.
(36) Stals, P. J. M.; Smulders, M. M. J.; Martín-Rapún, R.; Palmans, A. R. A.; Meijer, E. W. Asymmetrically Substituted Benzene-1,3,5-Tricarboxamides: Self-Assembly and Odd-Even Effects in the Solid State and in Dilute Solution. *Chem.—Eur. J.* **2009**, *15*, 2071−2080.
(37) Mes, T.; Cantekin, S.; Balkenende, D. W. R.; Frissen, M. M. M.; Gillissen, M. A. J.; De Waal, B. F. M.; Voets, I. K.; Meijer, E. W.; Palmans, A. R. A. Thioamides: Versatile Bonds to Induce Directional and Cooperative Hydrogen Bonding in Supramolecular Polymers. *Chem.—Eur. J.* **2013**, *19*, 8642−8649.
(38) Ten Eikelder, H. M. M.; Markvoort, A. J.; De Greef, T. F. A.; Hilbers, P. A. J. An Equilibrium Model for Chiral Amplification in Supramolecular Polymers. *J. Phys. Chem. B* **2012**, *116*, 5291−5301.
(39) Nakano, Y.; Hirose, T.; Stals, P. J. M.; Meijer, E. W.; Palmans, A. R. A. Conformational Analysis of Supramolecular Polymerization Processes of Disc-like Molecules. *Chem. Sci.* **2012**, *3*, 148−155.
(40) Tang, K.; Green, M. M.; Cheon, K. S.; Selinger, J. V.; Garetz, B. A. Chiral Conflict. The Effect of Temperature on the Helical Sense of a Polymer Controlled by the Competition between Structurally Different Enantiomers: From Dilute Solution to the Lyotropic Liquid Crystal State. *J. Am. Chem. Soc.* **2003**, *125*, 7313−7323.
(41) Palmans, A. R. A.; Vekemans, J. A. J. M.; Havinga, E. E.; Meijer, E. W. Sergeants-and-Soldiers Principle in Chiral Columnar Stacks of Disc-Shaped Molecules with C_3 Symmetry. *Angew. Chem., Int. Ed.* **1997**, *36*, 2648−2651.
(42) Smulders, M. M. J.; Filot, I. A. W.; Leenders, J. M. A.; Van Der Schoot, P.; Palmans, A. R. A.; Schenning, A. P. H. J.; Meijer, E. W. Tuning the Extent of Chiral Amplification by Temperature in a Dynamic Supramolecular Polymer. *J. Am. Chem. Soc.* **2010**, *132*, 611−619.
(43) ten Eikelder, H. M. M.; Adelizzi, B.; Palmans, A. R. A.; Markvoort, A. J. Equilibrium Model for Supramolecular Copolymerizations. *J. Phys. Chem. B* **2019**, *123*, 6627−6642.
(44) Lightfoot, M. P.; Mair, F. S.; Pritchard, R. G.; Warren, J. E. New Supramolecular Packing Motifs: π-Stacked Rods Encased in Triply-Helical Hydrogen Bonded Amide Strands. *Chem. Commun.* **1999**, 1945−1946.
(45) Filot, I. A. W.; Palmans, A. R. A.; Hilbers, P. A. J.; Van Santen, R. A.; Pidko, E. A.; De Greef, T. F. A. Understanding Cooperativity in Hydrogen-Bond-Induced Supramolecular Polymerization: A Density Functional Theory Study. *J. Phys. Chem. B* **2010**, *114*, 13667−13674.

DOI: 10.1021/acs.macromol.9b01502
Macromolecules 2019, 52, 7430−7438